

# Mitigating Backdoor Attacks in Federated Learning via Flipping Weight Updates of Low-Activation Input Neurons

Bin-bin Ding<sup>1</sup>, Peng-hui Yang<sup>2</sup>, Ze-qing Ge<sup>1</sup>, Sheng-jun Huang<sup>1</sup>

<sup>1</sup>College of Computer Science and Technology/Artificial Intelligence, Nanjing University of Aeronautics and Astronautics

<sup>2</sup>College of Computing and Data Science, Nanyang Technological University  
{dingbinb, Ze-qing Ge, Sheng-Jun Huang}@nuaa.edu.cn, {phyang.cs}@gmail.com

## Abstract

Federated learning enables multiple clients to collaboratively train machine learning models under the overall planning of the server while adhering to privacy requirements. However, the server cannot directly oversee the local training process, creating an opportunity for malicious clients to introduce backdoors. Existing research shows that backdoor attacks activate specific neurons in the compromised model, which remain dormant when processing clean data. Leveraging this insight, we propose a method called Flipping Weight Updates of Low-Activation Input Neurons (FLAIN) to defend against backdoor attacks in federated learning. Specifically, after completing global training, we employ an auxiliary dataset to identify low-activation input neurons and flip the associated weight updates. We incrementally raise the threshold for low-activation inputs and flip the weight updates iteratively, until the performance degradation on the auxiliary data becomes unacceptable. Extensive experiments validate that our method can effectively reduce the success rate of backdoor attacks to a low level in various attack scenarios including those with non-IID data distribution or high MCRs, causing only minimal performance degradation on clean data.

## Introduction

Federated Learning (FL) (McMahan et al. 2017), an emerging distributed machine learning framework, facilitates collaborative model training while preserving the privacy of decentralized data among clients. In recent years, FL has found extensive applications across various domains, including healthcare (Alzubi et al. 2022; Salim and Park 2022), financial services (Basu et al. 2021; Chatterjee, Das, and Rawat 2023), and intelligent transportation (Manias and Shami 2021; Zhao et al. 2022; Zhu et al. 2023b).

In FL, while privacy settings effectively protect participants' data privacy, they also prevent the server coordinating the global training from supervising the underlying processes, leading to a series of new security issues. A prominent concern is that malicious clients can manipulate local training data and model parameters to carry out backdoor attacks (Sun et al. 2019; Bagdasaryan et al. 2020; Fang and Chen 2023; Zhang et al. 2024). A backdoor attack embeds malicious behavior into the machine learning model, allowing it to function normally under standard conditions but to exhibit attacker-controlled behavior when specific triggers appear. As a result, the model maintains normal per-

formance on clean data while producing targeted incorrect results when exposed to the trigger data.

Currently, existing backdoor defense methods can be broadly categorized into two main types: mid-training defenses and post-training defenses. The former type of methods such as Krum (Blanchard et al. 2017), Bulyan (Mhamdi, Guerraoui, and Rouault 2018), and Trimmed Mean (Yin et al. 2018) mainly seek to identify and filter out malicious updates by scrutinizing discrepancies among the submitted data. These strategies aim to distinguish between benign and potentially malicious updates by detecting anomalies and inconsistencies. However, in scenarios involving Non-Independent and Identically Distributed (non-IID) data (Zhao et al. 2018; Zhang et al. 2021), the inherent variability in data distribution can amplify discrepancies among benign updates, thereby facilitating the evasion of detection by malicious updates. Recent research (Qin et al. 2024) confirms that benign and malicious updates exhibit a mixed distribution under non-IID conditions, with anomaly detection based on linear similarity failing to identify backdoors effectively (Fung, Yoon, and Beschastnikh 2018; Bhagoji et al. 2019; Xie, Koyejo, and Gupta 2020). RLR (Ozdayi, Kantarcioglu, and Gel 2021) is different from mainstream mid-training methods, which introduces a robust learning rate adjustment method to counter backdoor attacks, but it is still weakened under non-IID conditions and its effectiveness is also constrained by the malicious client ratio (MCR). Furthermore, existing research (Yin et al. 2018; Aramoon et al. 2021; Nguyen et al. 2021; Huang et al. 2023) highlights the critical need to keep the MCR below 50% in each training round to ensure the effectiveness of all these mid-training defensive mechanisms.

In post-training defenses, the necessity to identify update discrepancies across clients is eliminated, in contrast to the requirements of mid-training defenses. BadNets (Gu, Dolan-Gavitt, and Garg 2017) reveals that trigger samples activate a specific subset of neurons in compromised models, which otherwise remain dormant when exposed to clean inputs. These backdoor neurons often respond exclusively to trigger patterns (Zhu et al. 2023a) and exhibit high sensitivity to specific inputs (Zheng et al. 2022) or perturbations (Wu and Wang 2021). Building on this insight, subsequent studies (Liu, Dolan-Gavitt, and Garg 2018; Wang et al. 2019) demonstrate that pruning low-activation neu-

rons effectively mitigates backdoor attacks while preserving overall model performance. Such defenses concentrate on targeting and eliminating neurons with low-activation signals, thereby effectively preventing their activation by malicious inputs. Wu et al. (2020) applies pruning techniques for backdoor defense in FL and notes that the effectiveness of pruning depends on the attacker’s objectives. When backdoor and benign behaviors rely on the same neurons, pruning these neurons can significantly degrade the model’s performance on both malicious and clean data. The issue arises due to the neurons targeted for removal often playing crucial and essential roles in both backdoor attacks and benign inferences, which considerably reduces the model’s overall performance.

Drawing from the aforementioned research, we attempt to implement backdoor defenses that can eliminate the adverse effects of harmful neurons while preserving the function of normal neurons. In our method, we mainly focus on low-activation signals after they reach the fully connected layer. For these low-activation inputs, a potential strategy is to prune the associated neurons, thereby dispelling their contribution to the current layer’s output. Inspired by RLR (Ozdayi, Kantarcioglu, and Gel 2021), which utilizes a negative learning rate to flip the updates of low-confidence dimensions during training, we explore an alternative approach called Flipping Weight Updates of Low-Activation Input Neurons (FLAIN). Unlike pruning, which removes the output of these neurons, FLAIN adjusts their weights by flipping the updates, aiming to introduce larger perturbations to their contributions. In order to find out the best threshold for low-activation inputs, we introduce a performance-adaptive threshold, which increases in a short step each time, until the updated model’s performance drop becomes unacceptable. Extensive experiment results indicate that our method effectively eliminates backdoors with minimal performance degradation. We compare FLAIN with the baseline pruning method, and the results reveal that FLAIN adapts more effectively to a broader range of attack scenarios than pruning low-activation inputs, demonstrating superior defensive robustness.

Our main contributions can be summarized as follows:

- We explore a defense strategy for low-activation input neurons in the fully connected layer and propose a method, FLAIN, which mitigates backdoor attacks by flipping the weight updates associated with these neurons obtained during training.
- We introduce a performance-adaptive threshold for filtering low-activation inputs. The threshold increases in a short step each time and more neuron updates are flipped after each increase. The threshold will continue increasing until the updated model’s performance drop becomes unacceptable.
- We validate FLAIN’s consistent performance improvements across various settings, especially those with non-IID data distribution and high MCRs. The results demonstrate that FLAIN effectively lowers the success rate of backdoor attacks while preserving the model’s performance on clean data in these settings.

## Related Work

**Backdoor attacks in FL.** Common strategies for conducting backdoor attacks involve manipulating models to make specific predictions by embedding triggers within samples. These triggers can take various forms: numerical (Bagdasaryan et al. 2020), exploiting exact numerical values; semantic (Wang et al. 2020a), influencing predictions through subtle semantic cues; and even imperceptible forms (Zhang and Zheng 2024), which activate the backdoor despite being hard to detect. Xie et al. (2019) proposes decomposing a global trigger into localized variants across multiple malicious clients to enhance attack stealth.

**Mid-training defenses in FL.** In the quest to combat backdoor attacks, various defense mechanisms emerge. The Krum algorithm (Blanchard et al. 2017) focuses on selecting the global model by minimizing the sum of Euclidean distances to other local models. Similarly, the Trimmed Mean algorithm (Yin et al. 2018) mitigates the influence of outliers by discarding the highest and lowest values and calculating the average of the remaining data points. The Bulyan algorithm (Mhamdi, Guerraoui, and Rouault 2018) builds on this approach by first using Krum (Blanchard et al. 2017) to identify a more reliable subset of updates and then applying Trimmed Mean (Yin et al. 2018) for aggregation. RLR (Ozdayi, Kantarcioglu, and Gel 2021) utilizes robust learning rates to update the global model, applying a negative learning rate to dimensions with significant directional disparities to mitigate the impact of malicious updates. However, while these methods are effective in IID scenarios, their performance significantly diminishes in non-IID environments due to increased variability among client updates (Fung, Yoon, and Beschastnikh 2018; Xie, Koyejo, and Gupta 2020).

**Post-training defenses in FL.** For a backdoored model, certain neurons are activated by trigger samples but remain dormant with clean inputs. Pruning (Liu, Dolan-Gavitt, and Garg 2018; Wang et al. 2019) utilizes clean data to identify and remove these neurons, minimizing their impact during attacks. Wu et al. (2020) presents a strategy for FL where clients rank filters based on average activations from local data, and the server aggregates these rankings to prune the global model. Additionally, extreme weights are adjusted after pruning to enhance the robustness of the defense.

## Problem Setup

### Federated Learning

Suppose there are  $N$  clients in a FL system and the  $k$ -th client has a local dataset  $\mathcal{D}_k = \{(x_{k,i}, y_{k,i})\}_{i=1}^{n_k}$  of size  $n_k$ . The server manages client participation in each training round, with the global training objective defined as follows:

$$\mathbf{w}^* = \arg \min_{\mathbf{w}} \sum_{k=1}^N \lambda_k f(\mathbf{w}, \mathcal{D}_k), \quad (1)$$

$$f(\mathbf{w}, \mathcal{D}_k) = \frac{1}{n_k} \sum_{i=1}^{n_k} f(\mathbf{w}, (x_{k,i}, y_{k,i})), \quad (2)$$

where  $\mathbf{w}^*$  denotes the optimal global model parameters,  $f(\mathbf{w}, \mathcal{D}_k)$  represents the average loss computed over the dataset  $\mathcal{D}_k$  for client  $k$ ,  $(x_{k,i}, y_{k,i})$  denotes the  $i$ -th sample in  $\mathcal{D}_k$ , and  $\lambda_k$  indicates the weight of the loss for client  $k$ .

At the  $t$ -th federated training round, the server randomly selects a client set  $S_t$  where  $|S_t| = m$  and  $0 < m \leq N$ , and broadcasts the current model parameters  $\mathbf{w}_t$ . The selected clients perform local training and upload their updates  $\Delta \mathbf{w}_{t+1}^k$  to the server for global model aggregation. FedAvg (McMahan et al. 2017) uses a weighted averaging rule for aggregating client updates according to the volume of local data. The aggregation process is detailed as follows:

$$\mathbf{w}_{t+1} = \mathbf{w}_t + \alpha \cdot \frac{\sum_{k \in S_t} n_k \Delta \mathbf{w}_{t+1}^k}{\sum_{k \in S_t} n_k} \quad (3)$$

where  $\alpha$  denotes the global learning rate and  $\Delta \mathbf{w}_{t+1}^k$  represents the local training update from client  $k$ .

### Threat Model

Due to privacy constraints, the server lacks access to local training data and processes. Bagdasaryan et al. (2020) reveals vulnerabilities in FedAvg (McMahan et al. 2017), highlighting its susceptibility to backdoor attacks.

**Attacker’s Capabilities.** We assume that malicious attackers can perform white-box attacks, meaning they have access to both the training data and model parameters of compromised clients. However, these attackers do not have access to the data or model parameters of non-compromised clients, nor can they interfere with the aggregation process conducted by the server.

**Attacker’s Goals.** The backdoored model is engineered to predict a specific class for samples embedded with triggers. For instance, in image classification tasks, a backdoored model might misclassify images of airplanes containing triggers as birds, while accurately classifying other clean images. For any input  $x$ , the ideal output of the backdoored model  $\mathbf{M}_{\mathbf{w}}$  can be formulated as follows:

$$\mathbf{M}_{\mathbf{w}}(x) = \begin{cases} y, & \text{if } x \in \mathcal{D}_{clean}, \\ y_{target}, & \text{else,} \end{cases} \quad (4)$$

and the training objective can be formulated as follows:

$$\min_{\mathbf{w}} \underbrace{\mathbb{E}_{(x, y) \sim \mathcal{D}_{clean}} \ell(\mathbf{M}_{\mathbf{w}}(x), y)}_{\text{Average loss on clean data}} + \lambda \cdot \underbrace{\mathbb{E}_{(x', y_{target}) \sim \mathcal{D}_{poison}} \ell(\mathbf{M}_{\mathbf{w}}(x'), y_{target})}_{\text{Average loss on poisoned data}}, \quad (5)$$

where  $\ell$  is the loss function,  $y_{target}$  is the target label,  $\mathcal{D}_{clean}$  represents the clean dataset,  $\mathcal{D}_{poison}$  represents the poisoned dataset, and  $\lambda$  is a balancing parameter.

### Defense Model

**Defender’s Capabilities.** Consistent with prior research (Chen et al. 2020; Tan et al. 2020; Cao et al. 2020; Wang et al. 2020b), we assume that the server maintains a small auxiliary dataset, which is used to compute the activation inputs of the fully connected layer and to evaluate performance variations in the model.

**Defender’s Goals.** The backdoored model integrates information learned from both clean and trigger data, making it challenging to selectively remove backdoor information.

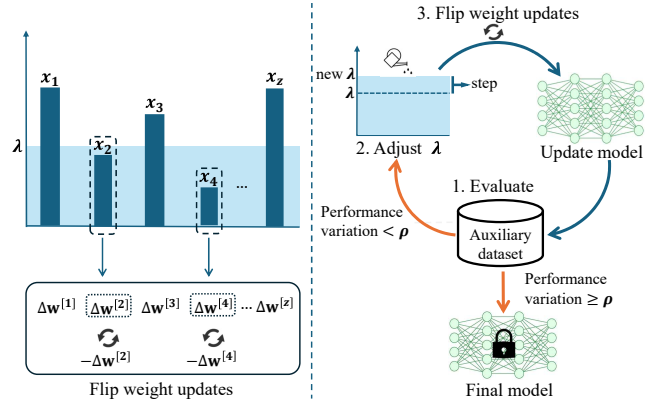


Figure 1: An illustration of FLAIN. The left side describes the process of flipping weight updates for neurons with average activation inputs below  $\lambda$ . The right side illustrates the loop of adaptively modifying the threshold  $\lambda$ , which consists of three steps: 1. comparing the model’s performance variations against the threshold  $\rho$ ; 2. incrementally increasing  $\lambda$  by a defined *step* size to expand the flipping interval; 3. flipping the weight updates and updating the model. The loop will continue until the model’s performance drop becomes larger than  $\rho$ , at which point the final model is obtained.

Therefore, the defender’s objectives are twofold: to reduce the model’s accuracy on trigger samples while maintaining its performance on the clean data.

## Methodology

In this section, we explain in detail the process of handling low-activation input neurons in the fully connected layer using flipping and the adaptive threshold, which is collectively called FLAIN.

### Flipping

**Activated inputs.** Consider a model that includes a fully connected layer  $\tau$  with  $z$  neurons, where the weight matrix  $\mathbf{W}$  is defined as  $\mathbf{W} = (\mathbf{w}^{[1]}, \mathbf{w}^{[2]}, \dots, \mathbf{w}^{[z]}) \in \mathbb{R}^{s \times z}$ . Each column vector  $\mathbf{w}^{[i]} = (w^{[i]1}, w^{[i]2}, \dots, w^{[i]s})^\top \in \mathbb{R}^s$  in  $\mathbf{W}$  represents the weights associated with the  $i$ -th neuron in layer  $\tau$ , where  $w^{[i]j}$  ( $j = 1, 2, \dots, s$ ) denotes the  $j$ -th element of the vector  $\mathbf{w}^{[i]}$ . Let  $\mathbf{x} = (x_1, x_2, \dots, x_z)^\top \in \mathbb{R}^z$  denote the inputs to layer  $\tau$ . These inputs are obtained by applying the ReLU activation function (Ramachandran, Zoph, and Le 2017) element-wise to the raw outputs from the preceding layer. Specifically, each component  $x_i$  ( $i = 1, 2, \dots, z$ ) of the vector  $\mathbf{x}$  is defined as  $x_i = \text{ReLU}(x'_i)$ , where  $x'_i$  represents the raw output from the preceding layer. The output  $\mathcal{H}(\mathbf{x})$  of layer  $\tau$  can be expressed as:

$$\begin{aligned} \mathcal{H}(\mathbf{x}) &= \mathbf{W}\mathbf{x} + \mathbf{b} \\ &= \begin{bmatrix} w^{[1]1}x_1 + w^{[2]1}x_2 + \dots + w^{[z]1}x_z + b_1 \\ w^{[1]2}x_1 + w^{[2]2}x_2 + \dots + w^{[z]2}x_z + b_2 \\ \dots \\ w^{[1]s}x_1 + w^{[2]s}x_2 + \dots + w^{[z]s}x_z + b_s \end{bmatrix} \end{aligned} \quad (6)$$

where  $\mathbf{b} = (b_1, b_2, \dots, b_s)^\top \in \mathbb{R}^s$  represents the bias vector of layer  $\tau$ .

**Flipping.** FLAIN offers a new approach for handling low-activation input neurons. In contrast to pruning that sets the weights of these neurons to 0, FLAIN modifies these weights by flipping the updates obtained during global training. Before training begins, the server initializes the global model parameters and records the initial weights of layer  $\tau$ :  $\mathbf{W}_0 = (\mathbf{w}_0^{[1]}, \mathbf{w}_0^{[2]}, \dots, \mathbf{w}_0^{[z]}) \in \mathbb{R}^{s \times z}$ .

Upon completing the entire global training, the server acquires layer  $\tau$ 's weights:  $\mathbf{W} = (\mathbf{w}^{[1]}, \mathbf{w}^{[2]}, \dots, \mathbf{w}^{[z]}) \in \mathbb{R}^{s \times z}$  and computes the weight updates:  $\Delta \mathbf{W} = \mathbf{W} - \mathbf{W}_0 = (\Delta \mathbf{w}^{[1]}, \Delta \mathbf{w}^{[2]}, \dots, \Delta \mathbf{w}^{[z]}) \in \mathbb{R}^{s \times z}$ . Employing an auxiliary dataset  $\psi$  that consists of clean data, the server assesses the model's performance, denoted as  $acc_0$ . At the same time, the server retrieves the activation input vector  $\mathbf{x} = (x_1, x_2, \dots, x_z)^\top \in \mathbb{R}^z$  for layer  $\tau$ , each  $x_i$  represents the average activation input of the whole auxiliary dataset for the  $i$ -th neuron in layer  $\tau$ . Then the server sets a threshold  $\lambda$ , and all  $x_i$  that are not larger than  $\lambda$  are collected into the set  $\mathcal{D}_{flip}$ . The detailed process of selecting the best threshold  $\lambda$  is described in the next subsection. Finally, the server flips  $\Delta \mathbf{w}^{[i]}$  to  $-\Delta \mathbf{w}^{[i]}$  and uses these flipped updates to update  $\mathbf{W}_0$ , which can be formulated as follows:

$$\mathbf{w}^{[i]*} = \begin{cases} \mathbf{w}_0^{[i]} - \Delta \mathbf{w}^{[i]}, & \text{if } x_i \in \mathcal{D}_{flip}, \\ \mathbf{w}_0^{[i]} + \Delta \mathbf{w}^{[i]}, & \text{else.} \end{cases} \quad (7)$$

The whole process of flipping is illustrated in the left side of Figure 1.

## Adaptive Threshold

The threshold  $\lambda$  proposed in the previous section highly determines the tradeoff between clearing backdoors and maintaining performance on clean data. To find out a better  $\lambda$  automatically, we propose an adaptive threshold selection method.

When firstly evaluating the fully-trained model on the auxiliary dataset, the server retrieves the average activation input vector  $\mathbf{x} = (x_1, x_2, \dots, x_z)^\top \in \mathbb{R}^z$  for layer  $\tau$  on the whole auxiliary dataset and identifies the minimum average activation value  $\mu \in \mathbf{x}$ . Then the server sets an initial threshold  $\lambda$  which is slightly larger than  $\mu$  and does the flipping process as described in the previous subsection. After updating the weights of layer  $\tau$  in the model from  $\mathbf{W}$  to  $\mathbf{W}^* = (\mathbf{w}^{[1]*}, \mathbf{w}^{[2]*}, \dots, \mathbf{w}^{[z]*}) \in \mathbb{R}^{s \times z}$ , the server assesses the current model's performance  $acc_1$  on the auxiliary dataset  $\psi$ . If the performance gap  $\epsilon = acc_0 - acc_1$  is less than a predetermined threshold  $\rho$ , the server increments  $\lambda$  by a  $step$  size and flip the weight updates again. This procedure is repeated until  $\epsilon$  exceeds the predefined threshold  $\rho$ , which means the performance drop exceeds the server's tolerance limit. The process of adaptively modifying the threshold is illustrated in the right side of Figure 1.

The details of the whole FLAIN method are summarized in Figure 1 and the pseudo codes are given in Algorithm 1.

---

## Algorithm 1: Flipping Weight Updates of Low-Activation Input Neurons (FLAIN)

---

**Input:** fully connected layer  $\tau$ 's initial weights  $\mathbf{W}_0$  and the number of neurons  $z$ ; model parameters  $\theta$  and layer  $\tau$ 's weights  $\mathbf{W}$  at the end of training; the  $step$  size; performance variation threshold  $\rho$ ; an auxiliary dataset  $\psi$ .

```

1:  $n_0 = \|\mathbf{W}\|_2$ 
2:  $\Delta \mathbf{W} = \mathbf{W} - \mathbf{W}_0$ 
3:  $\mu, \mathbf{x} = \text{Extract}(\theta, \psi)$ 
4:  $\lambda = \mu + step$ 
5:  $acc_0 = \text{Evaluate}(\theta, \psi)$ 
6: while True do
7:   for  $i = 1, 2, 3, \dots, z$  do
8:     if  $x_i \leq \lambda$  then
9:        $\mathbf{w}^{[i]*} = \mathbf{w}_0^{[i]} - \Delta \mathbf{w}^{[i]}$ 
10:    else
11:       $\mathbf{w}^{[i]*} = \mathbf{w}_0^{[i]} + \Delta \mathbf{w}^{[i]}$ 
12:    end if
13:  end for
14:   $\mathbf{W}^* = (\mathbf{w}^{[1]*}, \mathbf{w}^{[2]*}, \dots, \mathbf{w}^{[z]*})$ 
15:   $\theta^* = \text{Update}(\theta, \mathbf{W}, \mathbf{W}^*)$ 
16:   $acc_1 = \text{Evaluate}(\theta^*, \psi)$ 
17:  if  $\rho \leq acc_0 - acc_1$  then
18:     $n_1 = \|\mathbf{W}^*\|_2$ 
19:     $\mathbf{W}^* = \mathbf{W}^* \times \frac{n_0}{n_1}$ 
20:     $\theta^* = \text{Update}(\theta, \mathbf{W}, \mathbf{W}^*)$ 
21:  return  $\theta^*$ 
22: else
23:    $\lambda = \lambda + step$ 
24: end if
25: end while

```

**Output:** final model parameters  $\theta^*$ .

---

## Performance Evaluation

### Experiment Setup

**Training setup.** For our experiments, we use the Adam optimizer (Kingma and Ba 2014) with a learning rate of 0.001 and betas set to (0.9, 0.999). Each training round consists of local training for 1 epoch with a batch size of 256, while both the client sampling rate and the global learning rate are set to 1.

**Evaluation Metrics.** We utilize the following two metrics to assess the model's performance.

- **Attack Success Rate (ASR).** ASR measures the proportion of trigger samples that the model correctly classifies as the target class. This metric indicates the effectiveness of the backdoor attack, reflecting how well the attack can manipulate the model to produce the desired output for malicious inputs.
- **Natural Accuracy (ACC).** ACC quantifies the model's performance on untainted data, representing its effectiveness in standard classification tasks. This metric reflects how well the model generalizes to non-malicious inputs.

**Datasets and Models.** In the experiments, we utilize various datasets, including MNIST (Deng 2012), Fashion-MNIST

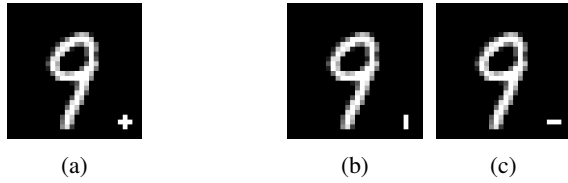


Figure 2: CBA pattern (a) and DBA pattern (b, c).

(Xiao, Rasul, and Vollgraf 2017), EMNIST (Cohen et al. 2017), and CIFAR-10 (Krizhevsky, Hinton et al. 2009).

- **MNIST** is a well-known dataset comprising handwritten digits (0-9), featuring 60,000 training images and 10,000 test images, each of which is  $28 \times 28$  pixels in grayscale. For experiments involving MNIST, we utilize a CNN architecture with 2 convolutional layers followed by 2 fully connected layers.
- **Fashion-MNIST (FMNIST)** serves as an alternative to MNIST, comprising grayscale images of 10 distinct clothing categories. It includes 60,000 training images and 10,000 test images, each sized at  $28 \times 28$  pixels. We employ a CNN architecture with 2 convolutional layers followed by 4 fully connected layers.
- **EMNIST** extends MNIST by including handwritten letters in addition to digits. Specifically, we use the “by-Class” partition, which contains 814,255 images distributed across 62 classes. The model architecture for EMNIST follows same structure as that used for MNIST.
- **CIFAR-10** is a widely-used image classification dataset comprising 60,000 color images divided into 10 categories, with each category containing 6,000 images, each sized  $32 \times 32$  pixels. We use a CNN network with 6 convolutional layers and 3 fully connected layers.

**Trigger Patterns.** We conduct experiments using both the CBA (Bagdasaryan et al. 2020) and DBA (Xie et al. 2019) patterns. Figure 2 illustrates the two different trigger patterns for class ‘9’ on MNIST.

- **Centralized Backdoor Attack (CBA):** Each malicious client possesses the complete trigger, which means they have full access to the entire trigger pattern used for backdoor attacks. The CBA pattern is evaluated across multiple datasets, including MNIST, EMNIST, FMNIST, and CIFAR-10.
- **Distributed Backdoor Attack (DBA):** The DBA pattern divides the complete trigger into partial patterns distributed across different clients, enhancing the attack’s stealth by reducing detection likelihood. We apply the DBA pattern specifically to CIFAR-10.

## Experiment Results

We set  $step$  as 0.001 and  $\rho$  no more than 0.03 for all settings. The auxiliary dataset  $\psi$  is drawn from the validation dataset, including 600 images from CIFAR-10, and 200 images each from MNIST, EMNIST, and FMNIST. We apply FLAIN to the first fully connected layer following the convolutional layers, and conduct comparative experiments with Pruning

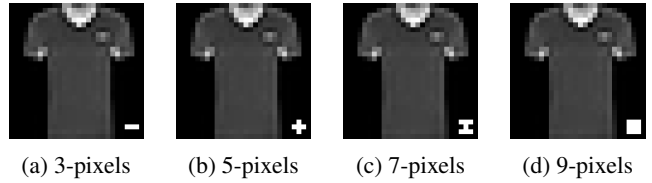


Figure 3: Various pixel backdoor patterns on FMNIST.

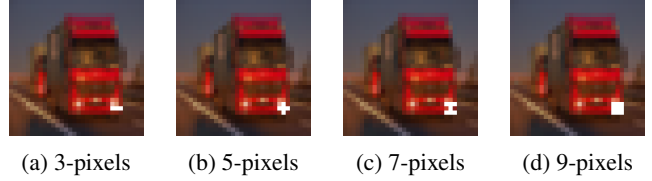


Figure 4: Various pixel backdoor patterns on CIFAR-10.

and RLR (Ozdayi, Kantarcioglu, and Gel 2021). For fair comparison, we also focus on the the first fully connected layer following the convolutional layers for Pruning.

**Attack tasks under IID.** We configure 10 clients with the MCR set to 40% and the poison data ratio (PDR) set to 30%. We define different attack tasks using the format (*Ground-truth label*, *Target label*). For this evaluation, the attack tasks are set to (0, 5), (0, 6), and (0, 7). As shown in Table 1, FLAIN, Pruning, and RLR effectively reduce the ASR to near 0 for certain tasks on MNIST, FMNIST, and EMNIST, with negligible impact on ACC. However, their performances vary significantly on CIFAR-10. Pruning seeks to enhance defense by removing additional neurons, resulting in a substantial decrease in ACC while the ASR remains elevated. RLR often applies a higher threshold to achieve a reduced ASR, leading to more dimensions receiving a negative learning rate, which negatively impacts model performance on the main task. In contrast, FLAIN consistently achieves an average ASR of 1.6% across the evaluated tasks, with only approximately 2% decrease in ACC.

**Attack tasks under non-IID.** We use a Dirichlet distribution ( $\alpha = 0.5$ ) to simulate non-IID data distribution scenarios commonly encountered in the real world, while maintaining all other settings consistent with IID conditions. Table 2 shows that under non-IID data distribution conditions, differences in data distribution result in more diverse client updates, which significantly undermines RLR’s effectiveness in defending against attacks on FMNIST and CIFAR-10. FLAIN and Pruning implement post-training backdoor defenses, thus avoiding the impact of dynamically distinguishing between malicious and benign updates during training. Comparatively, FLAIN outperforms Pruning, maintaining higher ACC and achieving lower ASR in the evaluated tasks.

**Different pixel backdoor patterns.** We train the model using 10 clients, with the MCR set to 40% and the PDR set to 50%, applying CBA to CIFAR-10. As shown in Figure 3 and Figure 4, we test different backdoor patterns by varying the number of trigger pixels (3, 5, 7, and 9) on FMNIST and CIFAR-10. The tasks are configured with FMNIST (1, 2)

Dataset		MNIST		FMNIST		EMNIST		CIFAR-10 <sub>DBA</sub>		
Attack	Defense	ASR↓	ACC↑	ASR↓	ACC↑	ASR↓	ACC↑	ASR↓	ACC↑	
0	5	no-Defense	0.949	0.992	0.991	0.901	1	0.854	0.974	0.837
		Pruning	0.001	<b>0.992</b>	0.021	0.890	<b>0</b>	<b>0.851</b>	0.392	0.770
		RLR	0.07	0.978	0.003	0.870	0.073	0.839	<b>0.005</b>	0.720
		FLAIN	<b>0</b>	<b>0.992</b>	<b>0</b>	<b>0.900</b>	<b>0</b>	0.850	0.019	<b>0.821</b>
	6	no-Defense	0.965	0.991	0.992	0.905	0.999	0.851	0.960	0.836
		Pruning	0.001	<b>0.991</b>	0.217	0.861	0.003	<b>0.849</b>	0.583	0.702
		RLR	<b>0</b>	0.980	0.084	0.862	0.063	0.838	<b>0.006</b>	0.712
		FLAIN	<b>0</b>	0.990	<b>0.027</b>	<b>0.897</b>	<b>0</b>	0.847	0.022	<b>0.820</b>
	7	no-Defense	1	0.989	0.989	0.904	0.999	0.856	0.972	0.820
		Pruning	0.001	<b>0.989</b>	0.054	0.885	<b>0</b>	0.854	0.606	0.705
		RLR	<b>0</b>	0.980	0.034	0.865	0.017	0.836	0.045	0.717
		FLAIN	<b>0</b>	<b>0.989</b>	<b>0</b>	<b>0.894</b>	<b>0</b>	<b>0.856</b>	<b>0.007</b>	<b>0.790</b>

Table 1: Results on IID data.  $\uparrow$  indicates larger values are better, and  $\downarrow$  indicates smaller values are better. **Bold** numbers are superior results.

Dataset		MNIST		FMNIST		EMNIST		CIFAR-10 <sub>CBA</sub>		
Attack	Defense	ASR↓	ACC↑	ASR↓	ACC↑	ASR↓	ACC↑	ASR↓	ACC↑	
0	5	no-Defense	1	0.989	0.989	0.899	0.999	0.844	0.976	0.785
		Pruning	<b>0</b>	<b>0.989</b>	0.340	0.884	0.001	0.843	0.197	0.746
		RLR	0.006	0.946	0.981	0.835	<b>0</b>	0.810	0.940	0.717
		FLAIN	<b>0</b>	<b>0.989</b>	<b>0.001</b>	<b>0.894</b>	<b>0</b>	<b>0.844</b>	<b>0</b>	<b>0.781</b>
	6	no-Defense	1	0.989	0.994	0.900	0.997	0.843	0.978	0.785
		Pruning	0.003	0.988	0.178	0.887	0.009	0.841	0.031	0.750
		RLR	0.002	0.950	0.120	0.828	<b>0.003</b>	0.806	0.954	0.710
		FLAIN	<b>0</b>	<b>0.989</b>	<b>0.005</b>	<b>0.895</b>	<b>0.003</b>	<b>0.843</b>	<b>0.001</b>	<b>0.783</b>
	7	no-Defense	1	0.989	0.989	0.902	0.985	0.844	0.979	0.798
		Pruning	0.001	<b>0.989</b>	0.063	0.886	0.001	0.843	0.121	0.702
		RLR	<b>0</b>	0.945	0.897	0.838	<b>0</b>	0.810	0.939	0.708
		FLAIN	<b>0</b>	<b>0.989</b>	<b>0.001</b>	<b>0.900</b>	<b>0</b>	<b>0.844</b>	<b>0.008</b>	<b>0.793</b>

Table 2: Results on non-IID data.  $\uparrow$  indicates larger values are better, and  $\downarrow$  indicates smaller values are better. **Bold** numbers are superior results.

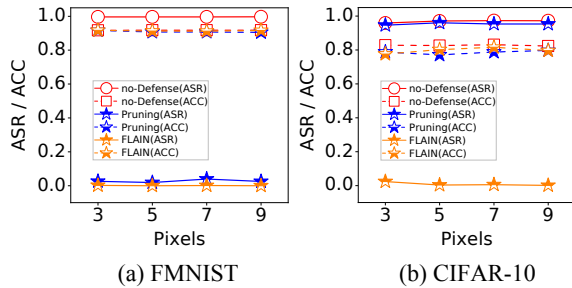


Figure 5: Performance across various pixel patterns.

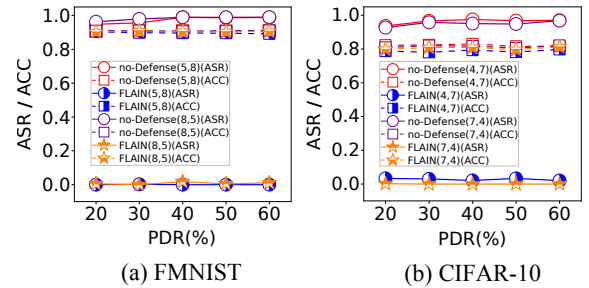


Figure 6: FLAIN's performance under different PDRs.

and CIFAR-10 (2, 1). Figure 5 shows that on FMNIST, the post-Defense ACC of FLAIN and Pruning remains relatively close across different backdoor patterns, although Pruning exhibits a slightly higher ASR. However, on CIFAR-10,

Pruning proves less effective, with a post-Defense ACC averaging 78.6% and an ASR as high as 95.3%. In contrast, FLAIN maintains an average ACC reduction of only about 3.2% across various backdoor patterns, while keeping the

Dataset		MNIST					
Num	MCR(%)	40		50		60	
	Defense	ASR↓	ACC↑	ASR↓	ACC↑	ASR↓	ACC↑
10	no-Defense	1	0.989	1	0.990	1	0.990
	Pruning	0	<b>0.989</b>	0	<b>0.990</b>	0	<b>0.990</b>
	RLR	0	0.968	0	0.970	0	0.975
	FLAIN	0	0.987	0	0.989	0	0.989
20	no-Defense	1	0.986	1	0.985	1	0.985
	Pruning	0	<b>0.986</b>	0	<b>0.985</b>	0	<b>0.985</b>
	RLR	0	0.963	0	0.968	0	0.953
	FLAIN	0	<b>0.986</b>	0	<b>0.985</b>	0	0.983

Table 3: Performance under various MCRs on MNIST.

Dataset		EMNIST					
Num	MCR(%)	40		50		60	
	Defense	ASR↓	ACC↑	ASR↓	ACC↑	ASR↓	ACC↑
10	no-Defense	0.973	0.853	0.992	0.854	0.997	0.854
	Pruning	0.004	<b>0.853</b>	0.003	<b>0.853</b>	0.001	<b>0.853</b>
	RLR	0.010	0.841	<b>0</b>	0.823	<b>0</b>	0.826
	FLAIN	<b>0</b>	<b>0.853</b>	<b>0</b>	<b>0.853</b>	<b>0</b>	<b>0.853</b>
20	no-Defense	0.957	0.845	0.992	0.845	0.995	0.845
	Pruning	0.001	0.844	0.001	<b>0.843</b>	0.004	<b>0.844</b>
	RLR	0.003	0.818	0.010	0.814	<b>0</b>	0.811
	FLAIN	<b>0</b>	<b>0.845</b>	<b>0</b>	<b>0.843</b>	<b>0</b>	0.843

Table 4: Performance under various MCRs on EMNIST.

ASR limited to approximately 0.8%.

**Impact of varying PDR.** We configure 15 clients and set the MCR to 40%. The CBA pattern applies to CIFAR-10, specific attack tasks on FMNIST [(5, 8), (8, 5)] and CIFAR-10 [(4, 7), (7, 4)]. PDR is set to 20%, 30%, 40%, 50%, and 60%, respectively. Figure 6 demonstrates that as PDR increases, the average ACC on FMNIST remains stable around 90%, with ASR values approaching 0. For CIFAR-10, the average ACC decreases by approximately 2% compared to the no-Defense model, while the ASR remains around 1%. Across different PDR settings, FLAIN effectively keeps the ASR at a minimal level while preserving the model’s performance on the main task.

**Diverse MCR settings.** The experiment uses 10 and 20 clients with the PDR set to 30%. We explore the impact of different MCR settings by configuring MCR to 40%, 50%, and 60%. Specific attack tasks include: MNIST (3, 6), FMNIST (6, 8), EMNIST (10, 20), and CIFAR-10 (4, 5). Based on the detailed analysis in Tables 3 - 6, FLAIN, Pruning, and RLR exhibit robust defense capabilities across MNIST, FMNIST, and EMNIST datasets, even as the number of compromised clients increases. However, on CIFAR-10, the effectiveness of RLR’s defense significantly declines as the MCR increases, particularly when the proportion of compromised clients reaches 50% and 60%. In these scenarios, the average

Dataset		FMNIST					
Num	MCR(%)	40		50		60	
	Defense	ASR↓	ACC↑	ASR↓	ACC↑	ASR↓	ACC↑
10	no-Defense	0.975	0.903	0.988	0.901	0.991	0.902
	Pruning	0.052	0.894	<b>0.003</b>	0.885	<b>0.001</b>	0.881
	RLR	0.015	0.852	0.021	0.773	0.027	0.767
	FLAIN	<b>0.001</b>	<b>0.901</b>	0.008	<b>0.900</b>	0.002	<b>0.888</b>
20	no-Defense	0.971	0.895	0.984	0.896	0.987	0.892
	Pruning	0.024	0.880	<b>0</b>	0.867	0.035	0.870
	RLR	0.027	0.779	0.024	0.774	0.043	0.776
	FLAIN	<b>0.001</b>	<b>0.888</b>	0.004	<b>0.894</b>	<b>0.003</b>	<b>0.891</b>

Table 5: Performance under various MCRs on FMNIST.

Dataset		CIFAR-10					
Num	MCR(%)	40		50		60	
	Defense	ASR↓	ACC↑	ASR↓	ACC↑	ASR↓	ACC↑
10 <sub>CBA</sub>	no-Defense	0.966	0.818	0.970	0.811	0.977	0.813
	Pruning	0.078	0.720	0.150	0.723	0.092	0.750
	RLR	<b>0.003</b>	0.715	0.649	0.696	0.796	0.673
	FLAIN	0.005	<b>0.814</b>	<b>0.001</b>	<b>0.804</b>	<b>0.002</b>	<b>0.796</b>
20 <sub>DBA</sub>	no-Defense	0.955	0.819	0.970	0.817	0.978	0.817
	Pruning	0.761	0.731	0.851	0.752	0.920	0.734
	RLR	0.315	0.698	0.497	0.678	0.798	0.670
	FLAIN	<b>0.017</b>	<b>0.800</b>	<b>0.012</b>	<b>0.798</b>	<b>0.016</b>	<b>0.799</b>

Table 6: Performance under various MCRs on CIFAR-10.

ACC decreases by 13.5%, while the ASR remains approximately 68.5%. Pruning exhibits better performance in systems with 10 participating clients under different MCR settings, but it still results in an average ACC loss of 8.3% and maintains the ASR around 10%. In contrast, FLAIN demonstrates stable defense performance across various MCR settings, with the maximum reduction in ACC not exceeding 2% and the ASR kept below 2%.

## Conclusion

In this paper, we introduce FLAIN, a backdoor defense method that flips the weight updates of low-activation input neurons. Given that the flipping process is highly sensitive to the threshold, we propose an adaptive threshold to automatically balance the tradeoff between eliminating backdoors and maintaining performance on clean data. The collaboration of flipping and the adaptive threshold supports the effectiveness of FLAIN. In evaluation tasks, FLAIN exhibits superior adaptability compared to direct pruning methods across a broader range of attack scenarios, including non-IID data distribution and high MCR settings. It consistently reduces backdoor efficacy while preserving the model’s accuracy on clean data. Future work will explore further enhancements to FLAIN, including its application in data-free scenarios and more complex models.

## References

- Alzubi, J. A.; Alzubi, O. A.; Singh, A.; and Ramachandran, M. 2022. Cloud-IIoT-based electronic health record privacy-preserving by CNN and blockchain-enabled federated learning. *IEEE Transactions on Industrial Informatics*, 19(1): 1080–1087.
- Aramoon, O.; Chen, P.-Y.; Qu, G.; and Tian, Y. 2021. Meta Federated Learning. *arXiv preprint arXiv:2102.05561*.
- Bagdasaryan, E.; Veit, A.; Hua, Y.; Estrin, D.; and Shmatikov, V. 2020. How to backdoor federated learning. In *Proceedings of the International Conference on Artificial Intelligence and Statistics*, 2938–2948.
- Basu, P.; Roy, T. S.; Naidu, R.; and Muftuoglu, Z. 2021. Privacy enabled financial text classification using differential privacy and federated learning. *arXiv preprint arXiv:2110.01643*.
- Bhagoji, A. N.; Chakraborty, S.; Mittal, P.; and Calo, S. 2019. Analyzing federated learning through an adversarial lens. In *Proceedings of the International Conference on Machine Learning*, 634–643.
- Blanchard, P.; El Mhamdi, E. M.; Guerraoui, R.; and Stainer, J. 2017. Machine learning with adversaries: Byzantine tolerant gradient descent. In *Advances in neural information processing systems*, volume 30.
- Cao, X.; Fang, M.; Liu, J.; and Gong, N. Z. 2020. Fltrust: Byzantine-robust federated learning via trust bootstrapping. *arXiv preprint arXiv:2012.13995*.
- Chatterjee, P.; Das, D.; and Rawat, D. B. 2023. Next generation financial services: Role of blockchain enabled federated learning and metaverse. In *Proceedings of the IEEE/ACM 23rd International Symposium on Cluster, Cloud and Internet Computing Workshops*, 69–74.
- Chen, Z.; Tian, P.; Liao, W.; and Yu, W. 2020. Zero knowledge clustering based adversarial mitigation in heterogeneous federated learning. *IEEE Transactions on Network Science and Engineering*, 8(2): 1070–1083.
- Cohen, G.; Afshar, S.; Tapson, J.; and Van Schaik, A. 2017. EMNIST: Extending MNIST to handwritten letters. In *Proceedings of the International Joint Conference on Neural Networks*, 2921–2926.
- Deng, L. 2012. The mnist database of handwritten digit images for machine learning research. *IEEE Signal Processing Magazine*, 29(6): 141–142.
- Fang, P.; and Chen, J. 2023. On the vulnerability of backdoor defenses for federated learning. In *Proceedings of the AAAI Conference on Artificial Intelligence*, volume 37, 11800–11808.
- Fung, C.; Yoon, C. J.; and Beschastnikh, I. 2018. Mitigating sybils in federated learning poisoning. *arXiv preprint arXiv:1808.04866*.
- Gu, T.; Dolan-Gavitt, B.; and Garg, S. 2017. Badnets: Identifying vulnerabilities in the machine learning model supply chain. *arXiv preprint arXiv:1708.06733*.
- Huang, S.; Li, Y.; Chen, C.; Shi, L.; and Gao, Y. 2023. Multi-metrics adaptively identifies backdoors in Federated learning. In *Proceedings of the IEEE/CVF International Conference on Computer Vision*, 4652–4662.
- Kingma, D. P.; and Ba, J. 2014. Adam: A method for stochastic optimization. *arXiv preprint arXiv:1412.6980*.
- Krizhevsky, A.; Hinton, G.; et al. 2009. Learning multiple layers of features from tiny images.
- Liu, K.; Dolan-Gavitt, B.; and Garg, S. 2018. Fine-pruning: Defending against backdoor attacks on deep neural networks. In *Proceedings of the International Symposium on Research in Attacks, Intrusions, and Defenses*, 273–294.
- Manias, D. M.; and Shami, A. 2021. Making a case for federated learning in the internet of vehicles and intelligent transportation systems. *IEEE Network*, 35(3): 88–94.
- McMahan, B.; Moore, E.; Ramage, D.; Hampson, S.; and y Arcas, B. A. 2017. Communication-efficient learning of deep networks from decentralized data. In *Proceedings of the International Conference on Artificial Intelligence and Statistics*, volume 54, 1273–1282.
- Mhamdi, E. M. E.; Guerraoui, R.; and Rouault, S. 2018. The Hidden Vulnerability of Distributed Learning in Byzantium. *arXiv preprint arXiv:1802.07927*.
- Nguyen, T. D.; Rieger, P.; Yalame, H.; Möllering, H.; Feridooni, H.; Marchal, S.; Miettinen, M.; Mirhoseini, A.; Sadeghi, A.-R.; Schneider, T.; and Zeitouni, S. 2021. FL-GUARD: Secure and Private Federated Learning. *arXiv preprint arXiv:2101.02281*.
- Ozdayi, M. S.; Kantarcioglu, M.; and Gel, Y. R. 2021. Defending against backdoors in federated learning with robust learning rate. In *Proceedings of the AAAI Conference on Artificial Intelligence*, 9268–9276.
- Qin, Z.; Chen, F.; Zhi, C.; Yan, X.; and Deng, S. 2024. Resisting Backdoor Attacks in Federated Learning via Bidirectional Elections and Individual Perspective. In *Proceedings of the AAAI Conference on Artificial Intelligence*, 14677–14685.
- Ramachandran, P.; Zoph, B.; and Le, Q. V. 2017. Searching for activation functions. *arXiv preprint arXiv:1710.05941*.
- Salim, M. M.; and Park, J. H. 2022. Federated learning-based secure electronic health record sharing scheme in medical informatics. *IEEE Journal of Biomedical and Health Informatics*, 27(2): 617–624.
- Sun, Z.; Kairouz, P.; Suresh, A. T.; and McMahan, H. B. 2019. Can you really backdoor federated learning? *arXiv preprint arXiv:1911.07963*.
- Tan, J.; Liang, Y.-C.; Luong, N. C.; and Niyato, D. 2020. Toward smart security enhancement of federated learning networks. *IEEE Network*, 35(1): 340–347.
- Wang, B.; Yao, Y.; Shan, S.; Li, H.; Viswanath, B.; Zheng, H.; and Zhao, B. Y. 2019. Neural cleanse: Identifying and mitigating backdoor attacks in neural networks. In *Proceedings of the IEEE Symposium on Security and Privacy*, 707–723.
- Wang, H.; Sreenivasan, K.; Rajput, S.; Vishwakarma, H.; Agarwal, S.; Sohn, J.-y.; Lee, K.; and Papailiopoulos, D. 2020a. Attack of the tails: Yes, you really can backdoor federated learning. In *Advances in Neural Information Processing Systems*, volume 33, 16070–16084.

Wang, Y.; Zhu, T.; Chang, W.; Shen, S.; and Ren, W. 2020b. Model poisoning defense on federated learning: A validation based approach. In *Proceedings of the International Conference on Network and System Security*, 207–223.

Wu, C.; Yang, X.; Zhu, S.; and Mitra, P. 2020. Mitigating backdoor attacks in federated learning. *arXiv preprint arXiv:2011.01767*.

Wu, D.; and Wang, Y. 2021. Adversarial neuron pruning purifies backdoored deep models. In *Advances in Neural Information Processing Systems*, volume 34, 16913–16925.

Xiao, H.; Rasul, K.; and Vollgraf, R. 2017. Fashion-mnist: a novel image dataset for benchmarking machine learning algorithms. *arXiv preprint arXiv:1708.07747*.

Xie, C.; Huang, K.; Chen, P.-Y.; and Li, B. 2019. Dba: Distributed backdoor attacks against federated learning. In *Proceedings of the International Conference on Learning Representations*.

Xie, C.; Koyejo, O.; and Gupta, I. 2020. Fall of empires: Breaking byzantine-tolerant sgd by inner product manipulation. In *Proceedings of the 35th Uncertainty in Artificial Intelligence Conference*, 261–270.

Yin, D.; Chen, Y.; Kannan, R.; and Bartlett, P. 2018. Byzantine-robust distributed learning: Towards optimal statistical rates. In *Proceedings of the International Conference on Machine Learning*, 5650–5659.

Zhang, H.; Jia, J.; Chen, J.; Lin, L.; and Wu, D. 2024. A3fl: Adversarially adaptive backdoor attacks to federated learning. *Advances in Neural Information Processing Systems*, 36.

Zhang, L.; and Zheng, B. 2024. FIBA: Federated Invisible Backdoor Attack. In *ICASSP 2024-2024 IEEE International Conference on Acoustics, Speech and Signal Processing (ICASSP)*, 6870–6874. IEEE.

Zhang, X.; Hong, M.; Dhople, S.; Yin, W.; and Liu, Y. 2021. Fedpd: A federated learning framework with adaptivity to non-iid data. *IEEE Transactions on Signal Processing*, 69: 6055–6070.

Zhao, J.; Chang, X.; Feng, Y.; Liu, C. H.; and Liu, N. 2022. Participant selection for federated learning with heterogeneous data in intelligent transport system. *IEEE Transactions on Intelligent Transportation Systems*, 24(1): 1106–1115.

Zhao, Y.; Li, M.; Lai, L.; Suda, N.; Civin, D.; and Chandra, V. 2018. Federated learning with non-iid data. *arXiv preprint arXiv:1806.00582*.

Zheng, R.; Tang, R.; Li, J.; and Liu, L. 2022. Data-free backdoor removal based on channel lipschitzness. In *Proceedings of the European Conference on Computer Vision*, 175–191.

Zhu, M.; Wei, S.; Shen, L.; Fan, Y.; and Wu, B. 2023a. Enhancing fine-tuning based backdoor defense with sharpness-aware minimization. In *Proceedings of the IEEE/CVF International Conference on Computer Vision*, 4466–4477.

Zhu, R.; Li, M.; Yin, J.; Sun, L.; and Liu, H. 2023b. Enhanced federated learning for edge data security in intelligent transportation systems. *IEEE Transactions on Intelligent Transportation Systems*, 24(11): 13396–13408.